Motional dynamics in proteins and nucleic acids control their function: revelation by time-domain fluorescence

G. Krishnamoorthy*

Department of Chemical Sciences, Tata Institute of Fundamental Research, Homi Bhabha Road, Mumbai 400 005, India

The complexity of biology world arises from the myriad of structures and their associated dynamics. The wealth of structural information available in biology has led to the realization that a complete understanding of biological processes requires information on dynamics apart from the knowledge on the high resolution structures. This realization has led to an explosion of information on dynamics from a variety of theoretical and experimental methods. Results from such studies show that the dynamics of small segments of biopolymers are anisotropic and position-dependent. Current efforts are focused on finding how this non-uniform dynamics form the basis of biological function. Various fluorescence-based methods have been designed to reveal biomolecular dynamics. They have a unique advantage due to their ultra-high sensitivity and selectivity. Furthermore, they cover a wide temporal range of femtosecond to seconds. In our laboratory we have been using time-domain fluorescence techniques for addressing issues related to dynamics of proteins, protein–DNA complexes, biomembranes and single living cells. In this review site-specific dynamics in nucleic acids and proteins are presented. Some of the counter-intuitive results on DNA dynamics arising from this work are likely to have relevance in the mechanism of formation of DNA–protein complexes. Site-specific dynamics in a RNA molecule reveals the mechanism of control of translation by the RNA. The internal motional dynamics of side-chains in proteins are found to be correlated with the dynamics of solvent around them. This finding addresses the importance of aqueous solvent in conferring activity to biopolymers in general.

Keywords: Motional dynamics, nucleic acids, proteins, time-domain fluorescence.

Motional dynamics in biology

WHILE a deep level of understanding of biology requires knowledge of chemistry, biology offers a fertile field of unsolved and exciting problems for those trained in chemistry. The seamless transition between chemistry and biology and the blurring of demarcation between them are best seen from the Nobel prizes in chemistry and the articles in several top journals in chemistry.

Biology works by apparently simple principles, but with complex chemical structures. Associated with complex structures are the 'dynamics' of bio-macromolecules such as proteins, nucleic acids, lipids and carbohydrates. As Richard Feynman observed 'Biology is all about wiggling and jiggling of atoms'. Thermally induced diffusive motion of biopolymers[1,2] is the source of dynamics in biological macromolecules. The amplitude and timescale of these fluctuations are quite anisotropic in space as expected from the anisotropy of the components of the biopolymer and the topology of its folding. Evolution has made effective use of the anisotropic nature of motional dynamics of biopolymers in endowing and modulating their function in the biological world. Thus, in recognition of the importance of dynamics, there is a perceptible transition from the concept 'structure $\rightarrow$ function' to the new concept '(structure + dynamics) $\rightarrow$ function'. This recognition has led to the application of a myriad of techniques, both experimental and theoretical, in unravelling dynamic aspects of biopolymers with the aim of gaining deeper understanding of the mechanisms of the biological world.

Molecular fluorescence when observed with a time-resolution of a few picoseconds becomes a powerful tool for revealing 'wiggling and jiggling' of groups of atoms in a macromolecule. By virtue of its sensitivity, selectivity and large temporal range, fluorescence spectroscopy has become one of the most revealing windows of biomolecular dynamics[3]. Of the several experimental methods available for studying macromolecular dynamics, fluorescence-based methods have the following advantages: (i) dynamics of a specific group or a segment of a massive macromolecular system can be observed without interference from the rest of the system; (ii) the timescale of observable dynamics covers a wide range of femtoseconds to seconds, and (iii) observations can be made under sparse levels of samples.

The dynamic nature of biomolecular structures, which is essential for their function, leads to structural heterogeneity. The diffusive motion of biopolymers, through a multitude of energy minima separated by barriers

*e-mail: gk@tifr.res.in

comparable to thermal energy in magnitude, is the cause of the conformational heterogeneity[2]. Due to its origin on dynamics, the apparent level of heterogeneity depends upon the time window used for observation by a physical technique. Techniques with large time windows result in averaging of structural parameters, whereas shorter windows produce an instantaneous snapshot of the structural states populating a distribution. The time window set by fluorescence-based techniques is linked to the excited state lifetime of the fluorophore, which lies generally in the range 10 ps to 10 ns. Since the timescale of large-scale and high-amplitude dynamics in macromolecules is generally in the range of nanoseconds and beyond[4], fluorescence methods capture essentially a snapshot of various structural forms present. The ensemble of structural forms of biomacromolecules could vary in their level of heterogeneity. While the spread in structural parameters is expected to be quite small for native and stable structures, partially structured intermediates encountered in situations such as protein-folding pathways are expected to have broader distributions of their structural characteristics. Furthermore, the amplitudes of local and segmental dynamics are expected to be non-uniform throughout the structure and probably related to functional domains of macromolecules. Hence the level of structural heterogeneity could also follow a non-uniform pattern. Such considerations demand that observations be made on fluorescence probes located at specific locations guided by information on the function of the system.

Motional dynamics in biopolymers can be categorized into the following three types: (i) Local or intrinsic dynamics which involves motion of a small group of atoms such as an indole ring in a protein, base in a nucleic acid or a covalently linked fluorophore with respect to the polymer chain to which it is attached. (ii) Dynamics of a small segment of the polymer with respect to the rest of the molecular system; this 'segmental dynamics' may be associated with several peptide or nucleotide units. (iii) Global tumbling dynamics of the entire macromolecular system. Each of these dynamic modes brings out useful information on the system. Local and segmental dynamics shows high level of anisotropy and position sensitivity, and is directly relevant for mechanisms of biological activity being controlled by dynamics. Global tumbling dynamics which is independent of the site of observation provides information on the overall size of the molecular system. Picosecond time-resolved fluorescence anisotropy measurements of either intrinsic fluorophores such as tryptophans or site-specifically labelled extrinsic fluorophores provide information on the dynamic modes mentioned above. In the sections to follow we shall see examples where time-resolved fluorescence of both intrinsic and extrinsic fluorophores has been used effectively to shed light on protein dynamics, protein folding dynamics, RNA dynamics and dynamics of DNA–protein complexes.

Structural information from fluorescence dynamics

Although time-domain fluorescence measurements are often thought of as providing information on dynamics of molecular systems, they also give us niche information on structural aspects of biomacromolecular systems. Access to structural information on systems for which standard structural tools such as X-ray crystallography and NMR are not feasible makes the fluorescence-based structural information useful and complementary. This section describes this aspect using some examples from our laboratory.

Folded and partially folded proteins

Proteins are known to exist in a variety of polymorphic structures apart from the commonly known native and unfolded states. Partially folded structures and molten globular forms encountered along the folding pathway, amorphous aggregates, protofibrils and fibrils are some of the polymorphic forms of proteins. While the native structures are well-characterize by the standard techniques, other forms lack sufficient structural details. Time-domain fluorescence offers specific structural information on proteins.

Global tumbling dynamics of proteins is governed by the hydrodynamics and hence the molecular volume. Rotational correlation time (ϕ) associated with this dynamic mode scales linearly with the molecular volume V($\phi = \eta V/kT = 1/6D$), where η is the viscosity and D is the rotational diffusion coefficient. Thus measurement of ϕ from fluorescence anisotropy decay kinetics[3,5] offers an effective way of addressing the level of aggregation of proteins and changes in their structural integrity. Table 1 gives typical examples of information, derived from rotational dynamics, on various structural forms of barstar, a single-domain protein (89 amino acids, Figure 1), which is used as a model protein in folding/unfolding and aggregation studies. Information on the structure derived from the rotational dynamics is also given in Table 1.

Unfolded proteins

Are proteins unfolded by chemical denaturants such as guanidine hydrochloride and urea completely unstructured random coils or have some residual structure? The answer to this question is essential for defining the starting point of folding. Residual structures present in the 'unfolded' ensembles[6], which might arise from sequence-specific propensity for native structure, might act as the seeding point for initiation of folding. Experimental techniques for studying structural aspects of unfolded proteins are quite limited in their number and scope. Time-resolved fluorescence-based methods offer information

Table 1. Rotational correlation times associated with the core tryptophan-53 in various stable structural forms of the protein barstar. The last column gives structural interpretation of the results

Structural form of barstar	Rotational correlation times, ϕ (ns) and (amplitude fraction)	Structural interpretation
Native (N) state (ref. 47)	5.1 ns (1.0)	Absence of fast (< 1 ns) local motion indicates rigid core in the native state
Unfolded (U) state (ref. 47)	0.76 ns (0.51) and 3.7 ns (0.49)	Presence of fast (0.76 ns) motion and segmental dynamics (3.7 ns) indicates flexible structure
Low pH, molten, globule-like form (A-form; ref. 5)	0.5 ns (0.45) and > 50 ns (0.55)	Fast (0.5 ns) motion indicates flexible core; very slow (> 50 ns) motion indicates aggregated form
High (12) pH, denatured form (D-state; ref. 47)	0.26 ns (0.50) and 2.6 ns (0.50)	Core is more flexible compared to neutral pH denatured form. Shows segmental flexibility
High (12) pH, salt-stabilized, compact form (P-state; ref. 47)	7.4 ns (1.0)	Absence of fast motion indicates rigid core; Slower global dynamics (7.4 ns) compared to the native state indicates swollen structure
Denaturation transition zone form (ref. 5)	1.5 ns (0.53) and 11.9 ns (0.47)	Fast (1.5 ns) motion shows flexible core; long (11.9 ns) global dynamics indicates partial unfolding leading to larger hydrodynamic radius
Protofibrils (refs 9, 10)	0.6 ns (0.37) and > 200 ns (0.63)	Fast (0.6 ns) motion shows flexibility; long (> 200 ns) global dynamics indicates large structure

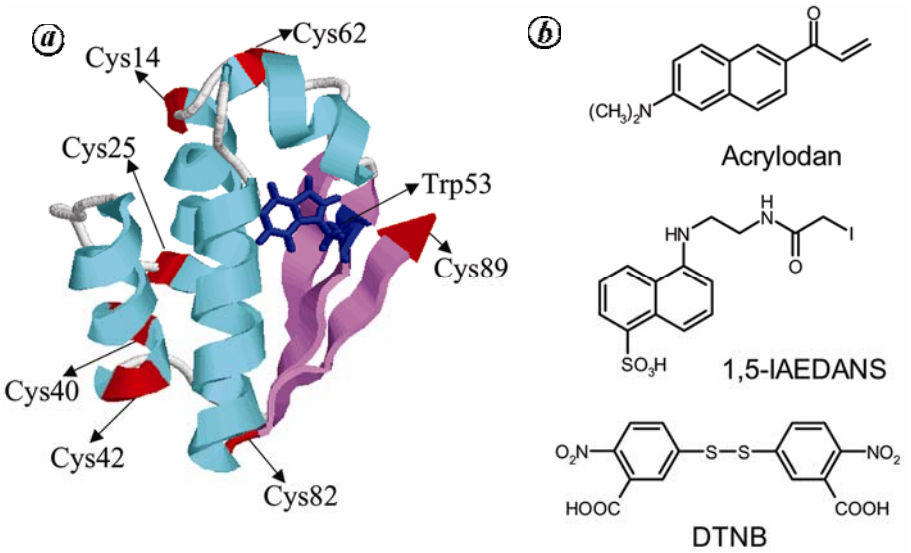

Figure 1. Model protein: ***a***, Structure of barstar protein showing the location of the core Trp53 and the various cysteine mutations. ***b***, Structures of fluorescence probes used to link at the cysteine side chain. Taken from Saxena *et al.*[7] with permission of the publishers.

on intramolecular distance, and distance distribution and site-specific motional dynamics of sidechains. This information could then be used to infer structural details as shown in the example below.

Several intramolecular distances estimated by time-resolved Fluorescence Resonance Energy Transfer (tr-FRET) measurements in barstar 'unfolded' by either GdnHCl or urea showed continuous expansion of the unfolded protein with increase in the concentration of the denaturants[7]. This observation is a clear indication for the presence of residual structure in the unfolded forms. Sequence-specific flexibility of the polypeptide chain (Figure 2), scored by site-specific fluorescence in the same protein also pointed towards the presence of structured regions in these unfolded forms[7]. The level of flexibility was higher towards the C-terminal end and increased with increase in the concentration of the denaturants. Such information would be vital in mapping the pathway of protein folding.

Protein aggregates and amyloid fibrils

Amyloid fibrils formed from aggregation of proteins form the class of structures for which the need of structural information is most acute. The scanty level of structural

information is due to the inability of standard structural tools such as NMR and X-ray crystallography in elucidating the structure of these molecular systems. Site-specific fluorescence labelling of proteins and time-domain fluorescence is an alternate structural tool as elaborated in the example given below.

Like several proteins, barstar forms soluble aggregates (called the A-form) at low (< 3) pH and when heated to ~ 60°C, the A-form transforms to curly structures called protofibrils which are the precursors to mature amyloid fibrils having a rigid, rod-like morphology[8,9]. A dansyl group-based fluorophore (IAEDANS, amino ethyl amino naphthalene sulphonic acid) was covalently attached to a single cysteine residue engineered at various locations along the polypeptide chain of this protein. Motional dynamics of this fluorophore was then monitored in protofibrils formed from these fluorescently labelled protein[9]. It was found that the amplitude associated with the local or internal motion (discussed earlier) of the fluorophore was dependent on the location along the polypeptide (Figure 3). This information was used to infer the following: (i) the aggregates formed at the low pH (the A-form) are the precursors to the protofibril and matured fibrils, and (ii) the N-terminal region of the polypeptide is more flexible compared to the rest suggesting that the C-terminal two-third of the peptide forms the core of the fibril. This model was also supported by measurement of solvent accessibility through dynamic fluorescence quenching of the fluorophore[9]. Solvent accessibility of the N-terminal one-third region is significantly higher compared to the rest of the sequence, indicating that this region is not structured in the fibril.

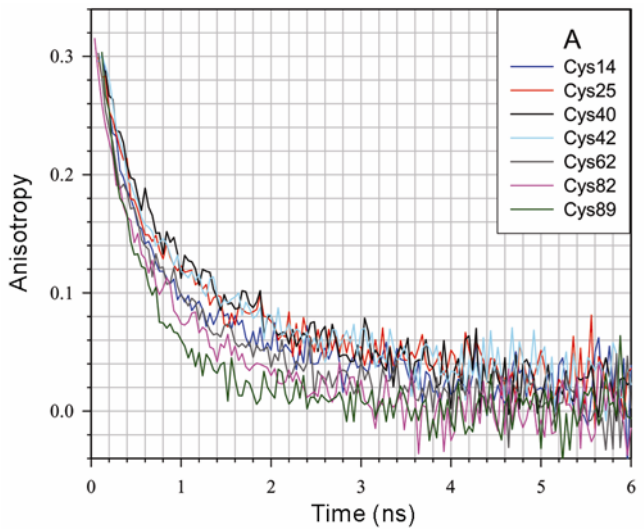

Figure 2. Revealing of residual structure in a 'unfolded' protein: Fluorescence anisotropy decay profiles of acrylodan-labelled single-cysteine variants of barstar unfolded in 8M urea. Rotational correlation times estimated from these curves vary as much as two-fold. This site-specific variation in the rotational motion of the fluorescence probe indicates the presence of residual structure in the 'unfolded' polypeptide. Taken from Saxena *e al.*[7] with permission of the publishers.

A more rigorous methodology based on fluorescence dynamics was also applied to elucidate the structure of the protofibrils. This novel methodology probes whether a polypeptide with a covalently attached fluorophore (called labelled peptide) can interact with another molecule of the same polypeptide without a fluorophore (called unlabelled peptide) to form the protofibril[10]. Differences in the hydrodynamic properties of the polypeptide aggregates scored through fluorescence anisotropy decay kinetics of the covalently attached fluorophore formed the basis of this methodology[10].

Firstly, it was shown that when a fluorophore was attached to certain locations in the polypeptide, the labelled and unlabelled peptides did not interact with other and each population went on to form their own aggregates and protofibrils (Figure 4). This remarkable result showed that the process of formation of protofibrils is akin to that of crystallization. In fact, microcrystals observed from fibril-forming short peptides[11] suggested that protein fibrils are very similar to crystals in its internal structure.

More interestingly, we observed that the inability of a mixture of labelled and unlabelled peptides to form co-fibril depend on the location of the fluorophore along the length of the polypeptide. This suggested to us a novel methodology of identifying the region(s) of the polypeptide involved in the formation of the core or the

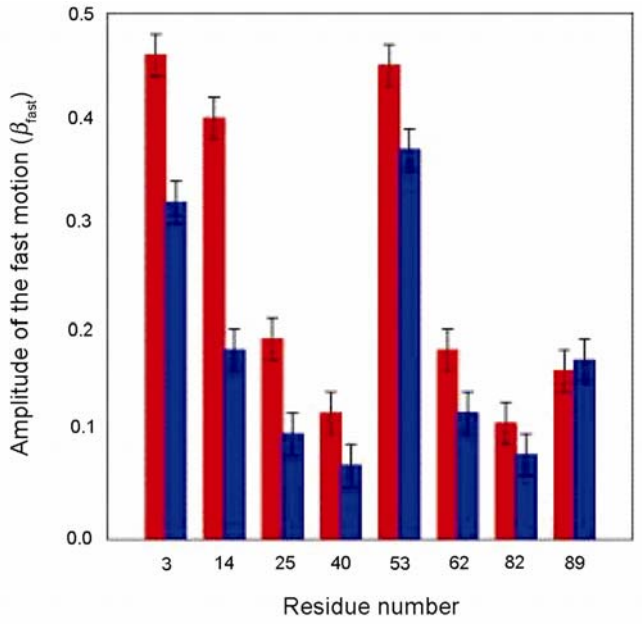

Figure 3. Structure from 'dynamics map': Map of the amplitude associated with the fast (internal) motion of the fluorophore covalently attached at various single-cysteine sites along the sequence of barstar in the A-form (red) and protofibril form (blue). The following observations are worth noting: (i) The C-terminal has larger amplitude, indicating that this regions is not a part of the rigid core of the structures. (ii) Similar amplitude profiles for the A-form and protofibrils suggest that the former could be the precursor for the latter, thus revealing the pathway of fibril formation. Taken from Mukhopadhyay *et al.*[9] with permission of the publishers.

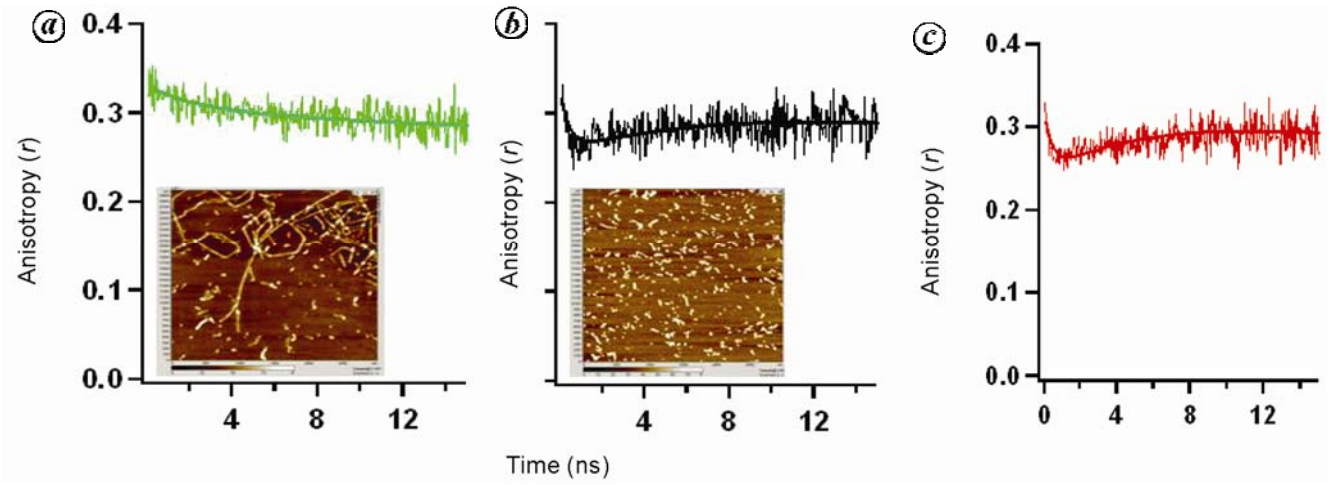

Figure 4. Internal structure of a protein fibril: Fluorescence anisotropy decay of the fluorophore IAEDANS covalently attached at Cys 82 of barstar (called labelled barstar) under various conditions. ***a***, Protofibrils formed from 50 μM of labelled barstar; ***b***, Protofibrils formed from 2 μM of the same sample, and ***c***, Protofibrils formed from a mixture of 2 μM of the labelled barstar and 48 μM of unlabelled barstar. (Insets in *a*, *b*) AFM images of the samples taken under liquid medium. The *X*-axes show time in ns. The profile in (***a***) indicates that the structures are very large having very slow tumbling dynamics (rotational correlation times > 200 ns). The profile in (***b***) is an unusual behaviour showing a 'dip-and-rise' characteristic of a mixture having at least two populations. This is interpreted as due to the presence of a mixture of monomers and very small oligomers[10]. A mixture of 2 μM of labelled barstar and 48 μM of unlabelled barstar (sample ***c***) could have given a profile similar to either (***a***) or (***b***). If the profile of (***c***) was similar to that of (***a***), the indication would be that the labelled and unlabelled barstar coaggregate and form co-fibrils. On the other hand if the profile for (***c***) is similar to that of (***b***), it would have meant that labelled and unlabelled proteins do not interact with each other and each population forms its own fibrils (for a more detailed explanation, Jha *et al.*[10]). The observation of profile (***c***) being similar to that of (***b***) indicates the inability of formation of co-fibril. This indicates that Cys 82 is a part of the structured core of the fibril. Information about other locations on the polypeptide was obtained in this way while making a map of the structure (Jha *et al.*[10] and Figure 5). Taken from Jha *et al.*[10] with permission of the publishers.

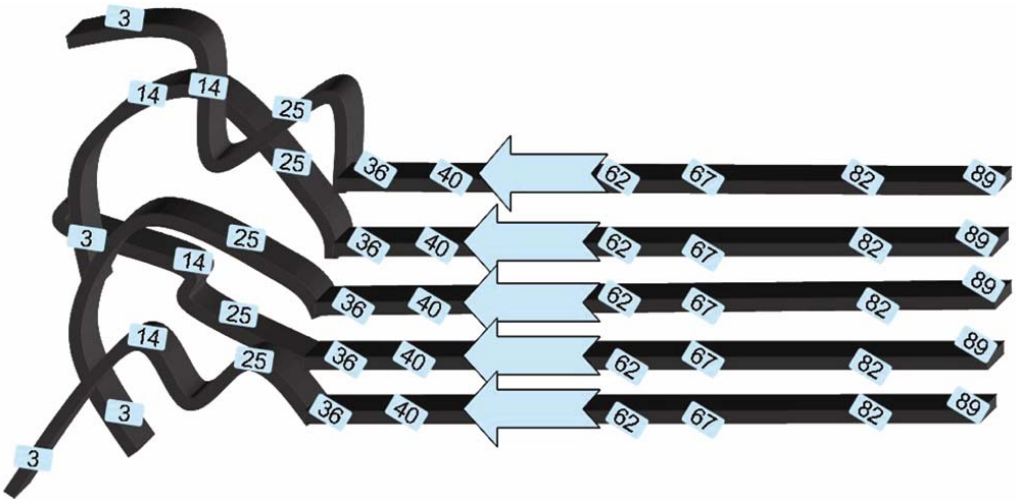

Figure 5. Fibril structure revealed: a schematic model for the structure of protofibrils of barstar. Self-complementary interactions in the rigid core region point toward a parallel organization of the polypeptide strands. The model shows that the entire C-terminal region, till its very end, participates in the specific inter-peptide interactions. This model was arrived at from the data similar to those shown in Figure 4. Taken from Jha *et al.*[10] with permission of the publishers.

ordered region of the fibril[11]. Fluorophore location-dependence of the ability/inability to form cofibrils, assayed through time-domain fluorescence anisotropy decay[11] was used to identify the core-forming region in the fibrils formed from barstar (Figure 5). This methodology could be applied to elucidate the structural features of other fibril-forming proteins in general.

Dynamics in nucleic acids

The information content of DNA and RNA is often assumed to be solely deposited in their sequence. While this assertion holds in a vast majority of situations, there are striking examples wherein the information retrieval from a sequence is modulated by the position of the

sequence with respect to an open end or even by the conformational states of their bound form[12]. Such extra-sequence information could primarily originate from position-dependence of structure and dynamics of DNA stretches. Despite the general realization that dynamics of DNA plays a vital role in DNA–protein interaction, the level of our understanding on nucleic acid dynamics[13,14] is rather limited. Furthermore, information on position-dependence of dynamics is even more stark by its sparseness[15,16]. In fact, several puzzles of molecular biology such as the mechanism by which ATP hydrolysis (but not binding alone) promotes homologous recombination[17] and mechanism of recognition of mismatches in newly synthesized DNA by the protein MutS[18] have answers based on sequence-specific dynamics in nucleic acids as elaborated below.

ATP hydrolysis-controlled DNA recombination

The RecA protein from *Escherichia coli* catalyses DNA recombination by reciprocal exchange of DNA strands between two homologous DNA molecules[17,19]. The overall process of RecA-catalysed strand exchange comprises several elementary steps involving intermediate complexes. Although RecA-mediated strand exchange involving short lengths of homology readily takes place in the presence of a poorly hydrolysable analogue of ATP (ATPγS), the same involving several hundred base pairs of homology tracts or the same interrupted by short sequence heterology barriers, critically requires RecA-mediated ATP hydrolysis for productive strand exchanges[20]. This requirement of ATP hydrolysis has largely remained as a puzzle.

Does the hydrolysis of ATP by the DNA-bound RecA endow the DNA any special property which might enable the strand exchange reaction? Does the DNA become flexible and dynamic, and thus help the process of homology search between the two DNA strands? In order to answer these questions, we monitored the segmental dynamics of DNA with the help of picosecond time-resolved fluorescence anisotropy decay kinetics of 2-aminopurine (2-AP, a fluorescent analogue of adenine, Figure 6)[21,22] incorporated in several constructs of DNA[23].

Double-stranded (ds) DNA is a rigid structure with a persistence length (average length of DNA which remains rigid and straight without taking a bend) of ~ 50 nm. In contrast, single-stranded (ss) DNA is highly flexible with a persistence length of < 1 nm. Hence ssDNA is expected to curl up significantly more compared to dsDNA. This

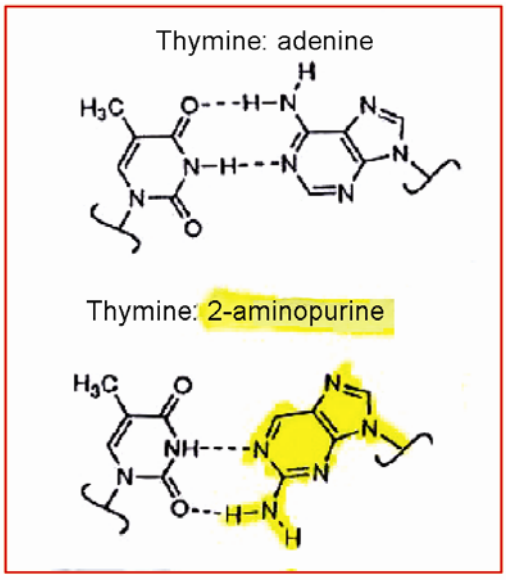

Figure 6. 2-Aminopurine (2-AP) as a fluorescence probe in DNA and RNA: Base-pairing scheme of 2-AP – thymine in comparison with the Watson–Crick base pair, A–T. The high fluorescence quantum yield of free 2-AP (> 0.6) gets quenched in nucleic acids and the level of quenching depends upon the near-neighbour stacking interactions. Thus the fluorescence of 2-AP becomes a sensitive reporter of the structure and dynamics of nucleic acids in general.

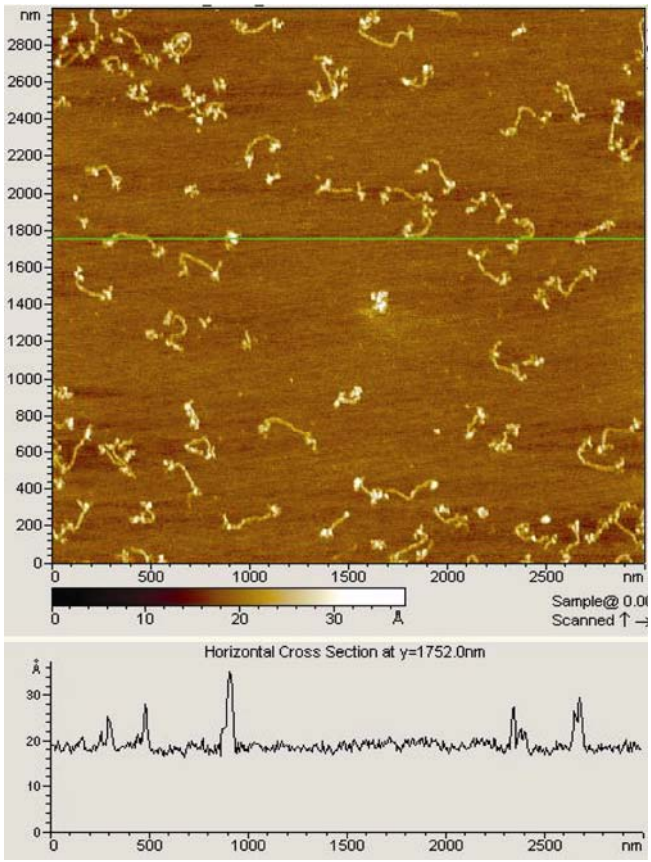

Figure 7. Segmental dynamics of DNA: Atomic force microscopic image of 3.46 kb linearized plasmid (pQE30) DNA treated with *Exo*III. Partial and controlled treatment with this enzyme results in 3′-single-stranded tailed ds-DNA. (Bottom panel) The heights corresponding to the green horizontal line in the main panel. Since the persistence length of ss-DNA is very small (< 1 nm) compared to that of ds-DNA (50 nm), these ss-tailed duplexes are seen having globular blobs at the ends of the more rigid ds-DNA. Thus, the difference in the segmental dynamics of ss-DNA and ds-DNA can be easily visualized.

can be best seen in the atomic force microscopic image of dsDNA with ss overhang regions (Figure 7). The DNA constructs we used in our experiments are quite short (30–60 base pairs), and hence they are expected to behave as rigid cylinders without any flexibility. 2-AP when incorporated into such DNA constructs displays two modes of motional dynamics, viz. (i) the internal or local motion of the fluorophore with respect to the macromolecule, and (ii) global tumbling dynamics of the entire DNA as expected (discussed earlier). Absence of segmental dynamics is also expected from these rigid structures (Figure 8). The motional dynamics of 2-AP is largely unaltered when RecA coats the DNA and also when the RecA-coated DNA was presented with ATPγS, a poorly hydrolysable analogue of ATP (Figure 8). However, when RecA-coated DNA was presented with ATP, the ensuing hydrolysis event leads to the generation of a novel dynamic mode which is reminiscent of segmental dynamics in polymers. This segmental motion with a rotational correlation time of ~8 ns (Figure 8) observed only during ATP hydrolysis is a strong indicator of ATP hydrolysis-induced flexibility of the DNA backbone[23]. Concerted hydrolysis of ATP by RecA[24] in the RecA–DNA filament could result in a standing wave of segmental dynamics in the filament. We hypothesize that this ATP hydrolysis-caused segmental dynamics is an important factor in aiding efficient strand exchange process as a result of pushing the branch migration through sequence impediments such as insertions/deletions. It is tempting to speculate that ATP hydrolysis-induced dynamics could be a general mechanism of enhancing biological activities which require substantial physical movement of segments of biopolymers.

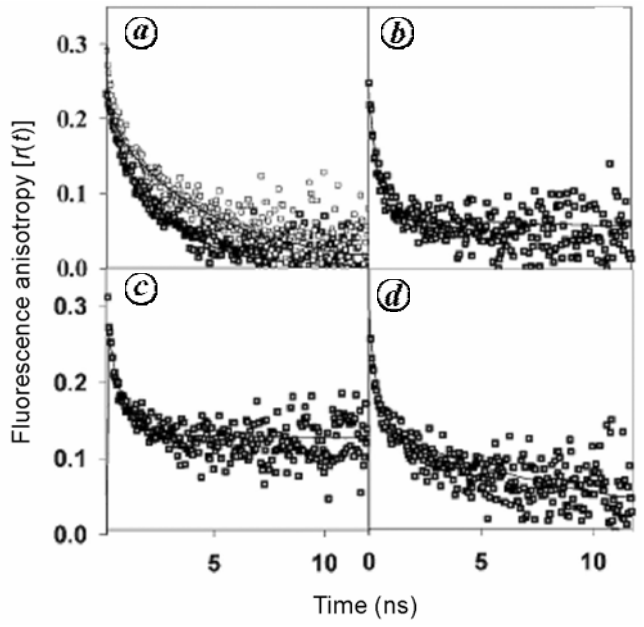

Figure 8. RecA-induced segmental dynamics in DNA: Typical curves of decay of fluorescence anisotropy of 2-AP incorporated in various DNA samples are shown. ***a***, 2AP–A_{30} (2-AP placed in a A-repeat ss-DNA of 30 nt) with ATPγS, a non-hydrolysable analogue of ATP. ***b***, 2AP-A_{30}–T-template duplex (T-template is a 31-mer repeat of T with flanking mixed sequence 18 nt long on either sides) with ATPγS. ***c***, 2AP–A_{30}-T-template duplex coated with RecA protein in ATPγS buffer, and ***d***, 2AP–A_{30}-T-template duplex coated with RecA in ATP regenerating condition. The segmental dynamics generated by the action of ATP hydrolysis in RecA-coated ds-DNA can be seen by the appearance of a new decay mode having a correlation time of ~8 ns (enhancement of the base slope in panels (***d***) compared to (***c***)). Taken from Ramreddy *et al.*[23] with permission of the publishers.

DNA base mismatch recognition

DNA mismatch repair system, an evolutionarily conserved biochemical pathway, plays an important role in regulating the genome by correcting base mismatches arising during the process of DNA replication including proof reading (error rate 10^{-6}–10^{-9}) (ref. 18). The first step in the mismatch repair is the identification of mismatches. This is a daunting task for the following reasons: (i) the mismatches are randomly spread at a rate of 1 in 10^6 to 10^9, and (ii) the mismatches are of a variety of types and shapes which might pose problem in identifying them, by a single protein, based on shape complementary nature such as lock-and-key mode seen in enzyme–substrate complexes. In *E. coli*, this task is performed by the protein MutS[25]. Several mechanisms for the recognition of mismatches have been proposed. These include

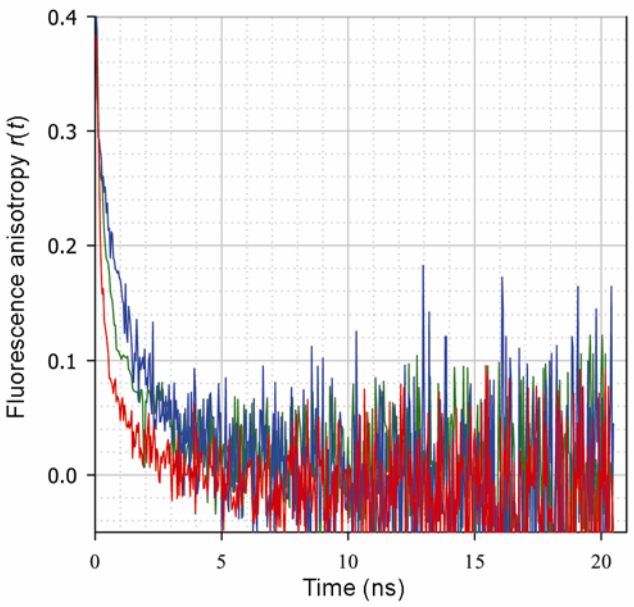

Figure 9. Enhancement in the base-pair dynamics at mismatched sites: Fluorescence anisotropy decay kinetics of 2-AP placed next to a mismatched G–T base pair (red) in a DNA construct[29] in comparison to a DNA sample with matched pair A–T (green). The dynamics next to another mismatched pair C–C (blue) is also shown. The rotational correlation times of these three traces are: 0.12, 0.35 and 0.34 ns respectively. Thus the dynamics felt close to the G–T base pair is nearly three-fold faster compared to that close to the A–T base pair. Taken from Nag *et al.*[29] with permission of the publishers.

the presence of kinks at the site of mismatch/deletion[26,27] and alteration in base dynamics[28]. As proposed for several situations of specific interaction between DNA and proteins, MutS is likely to bind to DNA non-specifically followed by one-dimensional search along the DNA. Such a mechanism helps in speeding up the search process as the search is done in one dimension rather than in three dimensions. While riding along the DNA, MutS would locate the site of base mismatch and reside at that location for a time longer than the residence time at any site of matched base pair, thus relaying the information on the location of the site of mismatch to other downstream players such as MutL, MutH, helicase, exonuclease and polymerase involved in the repair mechanism[25].

We addressed this issue of search/recognition mechanism of MutS by monitoring the motional dynamics around the site of mismatched base pairs (such as G–T, for example) with the help of fluorescence anisotropy decay kinetics of 2-AP located adjacent to the mismatched base pair in synthetic DNA constructs[29]. We observed a significant enhancement in the dynamics of 2-AP located as the near neighbour to a G–T mismatch when compared to the situation where the near neighbour was an A–T matched pair (Figure 9). Furthermore, we also observed the following: (i) The 2–3-fold enhancement in the dynamics of 2-AP next to the mismatched base pair when compared to matched pairs was seen only when 2-AP was the near neighbour; when 2-AP was moved 1–2 base pairs away, no enhancement was observed indicating that the mismatch-induced enhancement in dynamics is highly localized close to the site of mismatch. (ii) A C–C mismatch did not cause any significant enhancement in the dynamics unlike the G–T mismatch (Figure 9). When we noted that a C–C mismatch is not repaired as efficiently as a G–T mismatch in cells[30], we could conclude that the efficiency of recognition of a mismatch correlates with the extent of enhancement in the motional dynamics of the mismatched base pair.

How does MutS use the information of enhanced base pair dynamics in identifying the sites of mismatch? Once identified, MutS remains bound to that site for durations longer than the average residence time spent at other (matched base pair) sites while travelling along the length of the DNA. We speculate a mechanism based on the crystal structure of MutS–DNA complex[31] and our observation that the dynamics of 2-AP next to the mismatch site gets frozen when MutS is bound[29]. The crystal structure shows that the side chain of Phe36 of MutS gets stacked with the mismatched base pair[31]. This processes is reflected as dampened dynamics of the nearby 2-AP[29]. MutS binds to DNA initially in a non-specific manner and while scanning the length of the DNA, it probes the level of base pair dynamics. The base pair having faster dynamics (such as the G–T pair) helps in the insertion of Phe36 leading to efficient stacking interaction with the base pair. The stacking interaction offers extra binding energy resulting in longer residence time, thus enabling the downstream factors to carry out repair at that site. We propose that such a mechanism based on sensing any alteration in the level of dynamics would operate in several situations of protein–DNA interactions.

Dynamics in RNA switches

Apart from providing coding information for synthesis of proteins, mRNAs are emerging as regulators of expression of messages coded in the sequence[32]. The structure and dynamics of regions of mRNAs act as regulators[33]. These regulatory regions modulate the level of translation by a variety of modes such as binding to metabolites, temperature-sensitive alterations in local structure and dynamics, etc. Thus, once again, we encounter situations where polymer dynamics has profound effects in controlling physiological activity.

The Repression of heat Shock gene Expression (ROSE) element of mRNA present in the 5′-untranslated regions (UTR) of small heat-shock genes in many Gram-negative bacteria is known to function as a 'RNA thermometer' by controlling translation in a narrow temperature range of 30°C–42°C by blocking translation till 30°C and allowing it at 42°C and beyond, perhaps due to an unfolding transition of the ROSE hairpin motif[34].

We used site-specific fluorescence labelling and picosecond time-domain fluorescence spectroscopy to score the level of motional dynamics along the length of the RNA with the aim of unravelling the mechanism of temperature-sensitive translation[48]. The 'ROSE RNA' was site-specially labelled with 2-AP. Observables such as fluorescence lifetime, fluorescence anisotropy decay kinetics and dynamic fluorescence quenching revealed properties such as the level of base stacking, rotational motion of the bases, segmental dynamics of the backbone and the level of exposure of base to solvent. As expected, all the read-outs of 2-AP residue that were studied showed remarkable position dependence/sensitivity in the RNA sequence at 25°C. The striking result was the persistence of the same position dependence of the parameters even at 45°C, albeit at a measurably reduced levels (Figure 10). However the same position dependence was nearly 'wiped out' in the presence of urea where all intramolecular interactions in RNA are undone (Figure 10). These observations have prompted us to revise the existing model of ROSE RNA action: we now suggest that unlike as proposed earlier[35], the thermometer action of ROSE emanates not from its unfolding structural transition between 25°C and 45°C, but rather from its propensity to enhance structural dynamics without 'melting' the structure. We hypothesize that either the enhanced dynamics of the structure itself or its full melting due to an extrinsic factor (perhaps a protein interaction) might be the basis of its thermometer action[48]. Thus this constitutes another

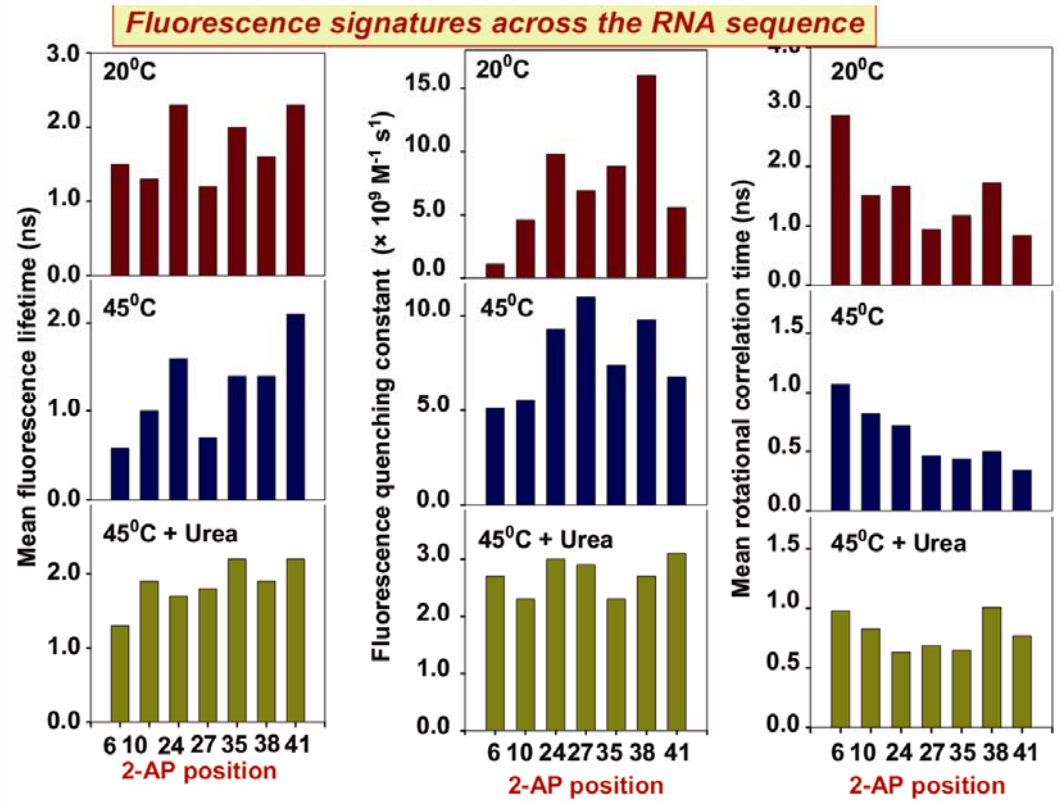

Figure 10. Site-specific dynamics in a 'RNA thermometer': 2-AP was incorporated at various locations of A in the 41-mer RNA sequence (5′-CUCGUACCCAUCUUGCUCCUUGGAGGAUUUGGCUAUGAGGA-3′). The histograms show (i) mean fluorescence lifetime, (ii) fluorescence quenching constant and (iii) mean rotational correlation time at 20°C, 45°C and 45°C with 8M urea. It can be seen that all the three read-outs show position dependence both at 20°C and 45°C, but largely position independence in the presence of urea due to loss of structure.

example wherein alteration in the level of dynamics is being used by nature to control a key physiological activity such as translation of a mRNA sequence.

Correlation between macromolecular dynamics and solvent dynamics

The examples detailed above are clear pointers to the assertion that proteins and other biological macromolecules are dynamic entities, and that the dynamics of various segments plays a major role in their functions[36–38]. The notion that solvent water plays a dominant role in dictating the dynamics has gained importance in recent years. The side chains of amino acid residues on the surface of a protein are hydrated resulting in several layers of bound water whose properties are the object of intense research efforts[39–42].

Frauenfelder and co-workers[40] have championed the notion that protein dynamics and hence, function are 'slaved' to solvent fluctuations. They have proposed the presence of two types of equilibrium fluctuations, namely α and β fluctuations, in proteins, in analogy to the fluctuations seen in glass-forming liquids. These fluctuations have been hypothesized to originate from fluctuations in the bulk solvent (α fluctuations) and in the hydration shell around the protein (β fluctuations). β fluctuations are thought to control internal motions of proteins. A recent experimental demonstration of a correlation between the β fluctuations and functional dynamics supports this hypothesis[40]. Although it has been argued extensively that macromolecular dynamics is slaved to solvent dynamics, experimental support for this hypothesis is scanty.

In this work, we address the question whether the 'solvation' dynamics is coupled to the local motional dynamics of the protein. Solvation dynamics was monitored by time-dependent dynamic Stoke shift (TDSS). TDSS was in turn estimated from femtosecond time-dependent emission spectra after being excited by 70 fs pulses in a fluorescence up-conversion/streak camera set-up[43]. Local (internal) motion of fluorophore covalently coupled to various sites in a protein was monitored by time-resolved fluorescence anisotropy measurements[3,5].

Barstar, the protein introduced above was site-specifically labelled with the fluorophore, acrylodan at different positions along the sequence (Figure 1). Barstar forms soluble aggregates (the A-form) at pH < 3, which have

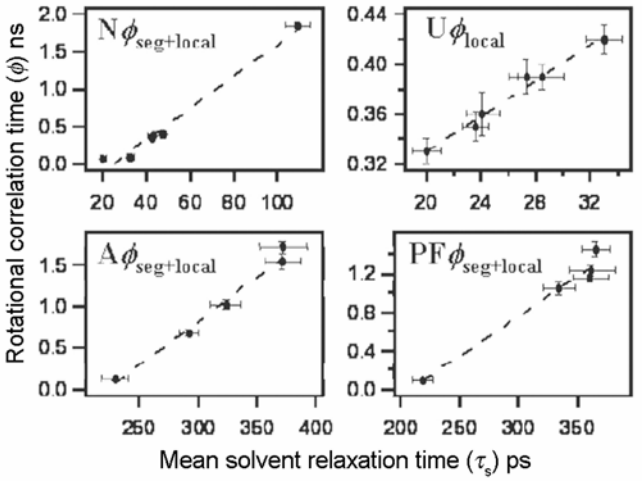

Figure 11. Correlation of solvation dynamics and internal dynamics of a protein: Each panel shows the correlation of the mean solvent relaxation time (τ_s) with segmental (ϕ_2) + local motion (ϕ_1) of the acrylodan-labelled mutant proteins (barstar) in the native (N), unfolded (U), A-form (A) and PF-forms (PF). Mean solvent relaxation time, τ_s is defined as $\tau_s = \tau_1\alpha_1 + \tau_2\alpha_2 + \tau_3\alpha_3$ (where $\alpha_1 + \alpha_2 + \alpha_3 = 1$). Internal dynamics of a protein is defined as $\phi_1\beta_1 + \phi_2\beta_2 = \phi_{seg+local}$ (where $\beta_1 + \beta_2 = 1$). The • symbols denote the actual values and dashed line denotes the best linear fit to the data. The error bars represent the standard deviations obtained from three separate sets of experiment. Taken from Jha *et al.*[46] with permission of the publishers.

been studied by fluorescence and NMR, and characterized as 160 kDa molten globule-like structures[44,45]. The A-form formed at low pH can be transformed into fibrillar aggregates at elevated temperatures[8,9]. The structure of protofibrils has been characterized using time-resolved fluorescence spectroscopy[10]. Each singly-labelled protein was studied in four structural forms, including the native protein, the unfolded protein, a soluble oligomer (A-form) and the protofibrillar form. The large number of samples enabled us to explore the correlations between 'solvation' dynamics and local protein dynamics[46].

Both the motional dynamics and solvent dynamics were found to be dependent upon the location of the probe as well as on the structural form of the protein. While the (internal) motional dynamics of the fluorophore occurs in the 0.1–3 ns time domain, the observed mean solvent relaxation times were in the range 20–300 ps (ref. 46). A strong positive correlation between these two dynamical modes was found in spite of the significant difference in their timescales (Figure 11). This observed correlation is a strong indicator of the coupling between solvent dynamics and the dynamics in the protein.

Conclusion

From the examples mentioned above, it must be clear by now that thermally driven motional dynamics in proteins and nucleic acids has a pivotal role in modulating biological activity of these macromolecules. Motional dynamics which is specific to a group of atoms in a biopolymer is quite varied in its timescale and extent, and this anisotropic characteristic of dynamics has been effectively used by nature in the evolution of living systems. Studies of the motional dynamics by a variety of spectroscopic tools such as time-domain fluorescence, as described in this article, will remain as a promising avenue in gaining knowledge on the mechanistic aspects of the biological world at the molecular level.

1. Krishnamoorthy, G., Fluorescence spectroscopy in molecular description of biological processes. *Indian J. Biochem. Biophys.*, 2003, **40**, 147–159.
2. Bryngelson, J. D., Onuchic, J. N., Socci, N. D. and Wolynes, P. G., Funnels, pathways and the energy landscape of protein folding. *Proteins*, 1995, **21**, 167–195.
3. Lakowicz, J. R., *Principles of Fluorescence Spectroscopy*, Springer, New York, 2006, 3rd edn.
4. Ishima, R. and Torchia, D. A., Protein dynamics from NMR. *Nature Struct. Biol*., 2000, **7**, 740–743.
5. Swaminathan, S., Nath, U., Udgaonkar, J., Periasamy, N. and Krishnamoorthy, G., Motional dynamics of a buried tryptophan reveals the presence of partially structured forms during denaturation of barstar. *Biochemistry*, 1996, **35**, 9150–9157.
6. Neri, D., Billeter, M., Wider, G. and Wuthrich, K., NMR determination of residual structure in a urea-unfolded protein, the 434-repressor. *Science*, 1992, **257**, 1559–1563.
7. Saxena, A., Udgaonkar, J. B. and Krishnamoorthy, G., Characterization of intra-molecular distances and site-specific dynamics in chemically unfolded barstar: Evidence for denaturant-dependent non-random structure. *J. Mol. Biol*., 2006, **359**, 174–189.
8. Gast, K. *et al.*, Effect of environmental conditions on aggregation and fibril formation of barstar. *Eur. Biophys. J*., 2003, **32**, 710–723.
9. Mukhopadhyay, S., Nayak, P. K., Udgaonkar, J. B. and Krishnamoorthy, G., Characterization of the formation of amyloid protofibrils from barstar by mapping residue-specific fluorescence dynamics. *J. Mol. Biol*., 2006, **358**, 935–942.
10. Jha, A., Udgonakar, J. B. and Krishnamoorthy, G., Characterization of the heterogeneity and specificity of inter-polypeptide interactions in amyloid protofibrils by measurement of site-specific fluorescence anisotropy decay kinetics. *J. Mol. Biol*., 2009, **393**, 735–752.
11. Sawaya, M. R. *et al.*, Atomic structures of amyloid cross-β spines reveal varied steric zippers. *Nature*, 2007, **447**, 453–457.
12. Shilatifard, A., Chromatin modification by methylation and ubiquitination: implication in the regulation of gene expression. *Annu. Rev. Biochem*., 2006, **75**, 243–269.
13. Shih, C. C. and Georghiou, S., Large amplitude fast motion in ds-DNA driven by solvent thermal fluctuations. *Biopolymers*, 2006, **8**, 450–463.
14. Zhang, Q., Sun, X., Watt, E. D. and Al-Hashim, H. M., Resolving the motional modes that code for RNA adaptation. *Science*, 2006, **311**, 653–656.
15. Larsen, O. F., van Stokkum, I. H., Gobets, B., van Grondelle, R. and van Amerongen, H., Probing the structure and dynamics of a DNA hairpin by ultrafast quenching and fluorescence depolarization. *Biophys. J*., 2001, **81**, 1115–1126.
16. Coman, D. and Russu, I. M., A nuclear magnetic resonance investigation of the energetics of base-pair opening pathways in DNA. *Biophys. J*., 2005, **89**, 3285–3292.
17. Roca, A. I. and Cox, M. M., RecA protein: structure, function and role in recombinational DNA repair. *Prog. Nucl. Acid Res. Mol. Biol*., 1997, **56**, 129–223.
18. Kunkel, T. A., DNA replication fidelity. *J. Biol. Chem*., 1992, **267**, 18251–18254.

19. Sen, S., Krishnamoorthy, G. and Rao, B. J., Real time fluorescence analysis of RecA filament: implications of base-pair fluidity in repeat realignment. *FEBS Lett*., 2001, **491**, 289–298.
20. Kim, J. I., Cox, M. M. and Inmam, R. B., On the role of ATP hydrolysis in RecA protein-mediated DNA strand exchange. II Four strand exchanges. *J. Biol. Chem*., 1992, **267**, 16438–16443.
21. Sowers, L. C., Fazakerley, G. V., Eritja, R., Kaplan, B. E. and Goodman, M. F., Base pairing and mutagenesis: observation of a protonated base pair between 2-aminopurine and cytosine in an oligonucleotide by proton NMR. *Proc. Natl. Acad. Sci. USA*, 1986, **83**, 5434–5438.
22. Nordlund, T. M., Andersson, S., Nilsson, L., Rigler, R., Graslund, A. and McLaughlin, L. W., Structure and dynamics of a fluorescent DNA oligomer containing the *Eco*RI recognition sequence: fluorescence, molecular dynamics and NMR studies. *Biochemistry*, 1989, **28**, 9095–9103.
23. Ramreddy, T., Sen, S., Rao, B. J. and Krishnamoorthy, G., DNA dynamics in RecA-DNA filaments: ATP hydrolysis-related flexibility in DNA. *Biochemistry*, 2003, **42**, 12085–12094.
24. Cox, J. M., Tsodikov, O. V. and Cox, M. M., Organized unidirectional waves of ATP hydrolysis within a RecA filament. *PLoS Biol*., 2005, **3**(2), e52.
25. Schofield, M. J. and Hsieh, P., DNA mismatch repair: molecular mechanisms and biological function. *Annu. Rev. Microbiol*., 2003, **57**, 579–608.
26. Lamers, M. H., Perrakis, A., Enzlin, J. H., Winterwerp, H. H. K., Wind, N. and Sixma, T. K., The crystal structure of DNA mismatch repair protein MutS binding to G.T mismatch. *Nature*, 2000, **407**, 711–717.
27. Obmolova, G., Ban, C., Hsieh, P. and Yang, W., Crystal structures of mismatch repair protein MutS and its complex with a substrate DNA. *Nature*, 2000, **407**, 703–710.
28. Isaacs, R. J., Rayens, W. S. and Spielmann, H. P., Structural differences in the NOE-derived structure of G–T mismatched DNA relative to normal DNA are correlated with differences in (13)C relaxation-based internal dynamics. *J. Mol. Biol*., 2002, **319**, 191–207.
29. Nag, N., Rao, B. J. and Krishnamoorthy, G., Altered dynamics of DNA bases adjacent to a mismatch: a cue for mismatch recognition by MutS. *J. Mol. Biol*., 2007, **374**, 39–53.
30. Modrich, P. and Lahue, R., Mismatch repair in replication fidelity, genetic recombination and cancer biology. *Annu. Rev. Biochem*., 1996, **65**, 101–133.
31. Schofield, M. J., Brownewell, F. E., Nayak, S., Du, C., Kool, E. T. and Hsieh, P., The Phe–X–Glu DNA binding motif of MutS. The role of hydrogen bonding in mismatch recognition. *J. Biol. Chem*., 2001, **276**, 45505–45508.
32. Batey, R. T. and Montange, R. K., Riboswitches: emerging themes in RNA structure and function. *Annu. Rev. Biophys*., 2008, **37**, 117–134.
33. Zhang, J., Lau, M. W. and Ferre-D'Amare, A. R., Ribozymes and riboswitches: modulation of RNA function by small molecules. *Biochemistry*, 2010, **49**, 9123–9131.
34. Nocker, A., Hausherr, T., Balsiger, S., Krstulovic, N. P., Hennecke, H. and Narberhaus, F., mRNA-based thermosensor controls expression of rhizobial heat shock genes. *Nucleic Acids Res*., 2001, **29**, 4800–4807.
35. Chowdhury, S., Maris, C., Allain, F. H.-T. and Narberhaus, F., Molecular basis for temperature sensing by an RNA thermometer. *EMBO J*., 2006, **25**, 2487–2497.
36. Berendsen, H. J. and Hayward, S., Collective protein dynamics in relation to function. *Curr. Opin. Struct. Biol*., 2000, **10**, 165–169.
37. Henzler-Wildman, K. and Kern, D., Dynamic personalities of proteins. *Nature*, 2007, **450**, 964–972.
38. Smock, R. G. and Gierasch, L. M., Sending signals dynamically. *Science*, 2009, **324**, 198–203.
39. Bhattacharyya, K., Nature of biological water: a femtosecond study. *Chem. Commun*., 2008, 2848–2857.
40. Frauenfelder, H. *et al*., A unified model of protein dynamics. *Proc. Natl. Acad. Sci. USA*, 2009, **106**, 5129–5134.
41. Golosov, A. A. and Karplus, M., Probing polar solvation dynamics in proteins: a molecular dynamics simulation analysis. *J. Phys. Chem. B*, 2007, **111**, 1482–1490.
42. Zhang, L., Wang, L., Kao, Y. T., Qiu, W., Yang, Y., Okobiah, O. and Zhong, D., Mapping hydration dynamics around a protein surface. *Proc. Natl. Acad. Sci. USA*, 2007, **104**, 18461–18466.
43. Iwamura, M., Takeuchi, S. and Tahara, T., Real-time observation of the photoinduced structural change of bis(2,9-dimethyl-1,10-phenanthroline)copper(I) by femtosecond fluorescence spectroscopy: A realistic potential curve of the Jahn–Teller distortion. *J. Am. Chem. Soc*., 2007, **129**, 5248–5256.
44. Swaminathan, R., Krishnamoorthy, G. and Periasamy, N., Similarity of fluorescence lifetime distributions for single tryptophan proteins in the random coil state. *Biophys. J*., 1994, **67**, 2013–2023.
45. Juneja, J., Bhavesh, N. S., Udgaonkar, J. B. and Hosur, R. V., NMR identification and characterization of the flexible regions in the 160 kDa molten globule-like aggregate of barstar at low pH. *Biochemistry*, 2002, **41**, 9885–9899.
46. Jha, A., Ishii, K., Udgaonkar, J. B., Tahara, T. and Krishnamoorthy, G., Exploration of the correlation between solvation dynamics and internal dynamics of a protein. *Biochemistry*, 2011, **50**, 397–408.
47. Rami, B. R., Krishnamoorthy, G. and Udgaonkar, J. B., Dynamics of the core tryptophan during the formation of a productive molten globule intermediate of barstar. *Biochemistry*, 2003, **42**, 7986–8000.
48. Kombrabail, M. H., Paul, S., Rao, B. J. and Krishnamoorthy, G., Mechanism of temperature-sensitive RNA translation revealed by site-specific fluorescence dynamics. *Proc. Trombay Symp. Radiation and Photochem*., 2010, **II**, 291–293.

ACKNOWLEDGEMENTS. I thank Profs Jayant Udagonkar, B. J. Rao and Tahei Tahara; Drs Bhadresh Rami, Nabanita Nag, T. Ramreddy, Anjali Jha, Kunihiko Ishii, Anoop Saxena and Samrat Mukhopadhyay and Ms Mamata Kombrabail for their collaboration in the work described here. I also thank Prof. N. Periasamy for providing the software used in the analysis of time-domain fluorescence data and his advice for its effective usage. The author is a recipient of the J. C. Bose National Research Fellowship from the Government of India.